Biogeosciences, 10, 7847–7862, 2013
www.biogeosciences.net/10/7847/2013/
doi:10.5194/bg-10-7847-2013

Biogeosciences Open Access

Technical Note: Simultaneous measurement of sedimentary N_2 and N_2O production and a modified ^{15}N isotope pairing technique

T.-C. Hsu[1,2] **and S.-J. Kao**[2,3,*]

[1]Earth System Science Program, Taiwan International Graduate Program, Academia Sinica, Taipei, Taiwan
[2]Research Center for Environmental Changes, Academia Sinica, Taipei, Taiwan
[3]State Key Laboratory of Marine Environmental Science, Xiamen University, Xiamen, China
[*]present address: Research Center for Environmental Changes, Academia Sinica, 128 Sec. 2, Academia Rd., Nankang Taipei, 115 ROC, Taiwan

Correspondence to: S.-J. Kao (sjkao@gate.sinica.edu.tw)

Received: 31 March 2013 – Published in Biogeosciences Discuss.: 17 April 2013
Revised: 14 September 2013 – Accepted: 1 October 2013 – Published: 3 December 2013

Abstract. Dinitrogen (N_2) and/or nitrous oxide (N_2O) are produced through denitrification, anaerobic ammonium oxidation (anammox) or nitrification in sediments, of which entangled processes complicate the absolute rate estimations of gaseous nitrogen production from individual pathways. The classical isotope pairing technique (IPT), the most common ^{15}N nitrate enrichment method to quantify denitrification, has recently been modified by different researchers to (1) discriminate between the N_2 produced by denitrification and anammox or to (2) provide a more accurate denitrification rate under considering production of both N_2O and N_2. In case 1, the revised IPT focused on N_2 production being suitable for the environments of a low N_2O-to-N_2 production ratio, while in case 2, anammox was neglected. This paper develops a modified method to refine previous versions of IPT. Cryogenic traps were installed to separately preconcentrate N_2 and N_2O, thus allowing for subsequent measurement of the two gases generated in one sample vial. The precision is better than 2 % for N_2 (m/z 28, m/z 29 and m/z 30), and 1.5 % for N_2O (m/z 44, m/z 45 and m/z 46). Based on the six m/z peaks of the two gases, the ^{15}N nitrate traceable processes including N_2 and N_2O from denitrification and N_2 from anammox were estimated. Meanwhile, N_2O produced by nitrification was estimated via the production rate of unlabeled $^{44}N_2O$. To validate the applicability of our modified method, incubation experiments were conducted using sediment cores taken from the Danshuei Estuary in Taiwan. Rates of the aforementioned nitrogen removal processes were successfully determined. Moreover, N_2O yield was as high as 66 %, which would significantly bias previous IPT approaches if N_2O was not considered. Our modified method not only complements previous versions of IPT but also provides more comprehensive information to advance our understanding of nitrogen dynamics of the water–sediment interface.

1 Introduction

Nitrate as fertilizer that ends up in the environment, polluting waterways and the coastal zone or accumulating in soils and groundwater, will be transformed to dinitrogen (N_2) and nitrous oxide (N_2O) gases via denitrification, anammox and nitrification processes and thus be removed from the environments (Joye and Anderson, 2008). N_2O is a strong greenhouse gas, and net oceanic emission accounts for one-third of atmospheric N_2O flux (Bange, 2006). N_2O production in the ocean may be further increased by increasing anthropogenic nitrogen inputs, exacerbating coastal eutrophication and global warming (Naqvi et al., 2010). Sediment–water interface is a major locus for nitrogen removal in aquatic environments. To better predict dynamic nitrogen cycles in future, it is critical to explore the processes and regulation factors of nitrogen removal and N_2O emission through the sediment–water interface.

The ^{15}N tracer-based methods have been applied widely in nitrogen cycle studies in terrestrial and aquatic environments (Groffman et al., 2006). These methods provide a

straightforward approach to quantify denitrification rates by adding ^{15}N-labeled NO_3^- ($^{15}NO_3^-$) and then measuring the gaseous production after incubations. Since ^{15}N-labeled N_2 ($^{15}N_2$) and/or N_2O ($^{15}N_2O$) will be generated at the same time, simultaneous analysis of $^{15}N_2$ and $^{15}N_2O$ is critical to single out the respective contribution from the different processes in the complicated nitrogen reaction web. However, few separate measurements have been performed for $^{15}N_2$ and $^{15}N_2O$ (Dong et al., 2006; Minjeaud et al., 2008; Trimmer et al., 2006; Trimmer and Nicholls, 2009). To our knowledge, simultaneous dual measurements have not yet been performed in aquatic environments due to methodological difficulties, though several have been conducted in soil studies (Bergsma et al., 2001; Spott et al., 2006; Stevens et al., 1993).

In aquatic environments, ^{15}N nitrate enrichment techniques, e.g., the isotope pairing technique (IPT), are often used to study nitrate removal processes. Following the original development of IPT by Nielsen (1992), several modified versions were proposed to accommodate anammox or to resolve specific nitrogen removal processes in sediments (Fig. 1). The original version of IPT ($IPT_{classic}$, yellow plate in Fig. 1) was used to estimate the genuine N_2 gas production rate ($P_{14-classic}$) defined as an estimate of $^{14}N_2$ production as it would have occurred without the addition of a ^{15}N tracer, i.e., N_2 production by reactions utilizing $^{14}NO_3^-$. However, the recently discovered anammox was not included. Based on $IPT_{classic}$, Risgaard-Petersen et al. (2003) and Trimmer et al. (2006) proposed IPT_{ana} to allow for additional estimation of anammox (yellow and blue plates in Fig. 1). The above methods only focused on N_2 production by denitrification ($IPT_{classic}$) or by denitrification and anammox (IPT_{ana}). The $^{15}N_2O$ production was indeed quantified in Trimmer et al. (2006) to derive the ratio between $^{14}NO_3^-$ and $^{15}NO_3^-$, but they did not introduce N_2O production into the denitrification rate estimation because it was low and ignorable (see Sect. 3.1). During the same period, Master et al. (2005) proposed an alternative approach, IPT_{N_2O}, which considered both N_2 and N_2O from denitrification (see the pink and yellow plates in Fig. 1), but their method did not account for anammox. Rather, their work focused on the theory without providing experimental data.

We installed a preconcentration system to trap and release N_2O and N_2 separately for isotope measurements. To overcome the aforementioned shortcomings of various IPT versions, we reassemble the formulae of former versions of IPT. Our modified method, IPT_{anaN_2O}, considers both N_2O production and anammox, allowing for us to determine the absolute rate of each individual N removal pathway among complicated transformation processes, and thus to gain better insight into the full scheme of the nitrogen reaction web (Fig. 1).

2 Instrument setup and evaluations

A program-controlled trap-and-release preparation line was constructed and connected to an isotope-ratio mass spectrometer (IRMS) to facilitate the simultaneous quantification of stable isotope compositions of N_2 and N_2O extracted from a single vial. Since the concentration of N_2 is often 3 to 5 orders of magnitude higher than N_2O in aquatic environments, we need to enlarge the analytical capacity of our instrument system. An extra head amplifier was added to each of the three detectors in the IRMS to widen the detection range, and an adjustable N_2 divider (open split to atmosphere) was installed in the preparation system to reduce N_2 inflow into the IRMS. Through this modified system, the genuine production of N_2 and N_2O from denitrification and anammox ($P_{14-anaN_2O}$) – i.e., the ^{14}N-N_2 and ^{14}N-N_2O production rate as it would have occurred without the addition of $^{15}NO_3^-$ – can be derived from the modified IPT formulae. The rate of N_2O formation via nitrification could be estimated as well.

2.1 Preconcentration system and instrument modification

The preconcentration system (Fig. 2) was added to an existing combination of equipment including a GC-Pal autosampler (CTC Analytics, LEAP Technologies), a GasBench II embedded with a PoraPlot Q GC column (25 m) and an IRMS (Thermo Delta^{plus} Advantage). The sample preparation line was composed of three two-position rotary valves (V1–V3, Vivi Valco prod. No. A4C8WT) program-controlled by Isodat software. We followed Mcllvin and Casiotti (2010) using the two-way concentric needle for the autosampler to flush and retrieve gases out of the vial. Although two Nafion gas dehumidifying tubes had originally been installed by the manufacturer on the GasBench II, we added an extra chemical column (12 inch glass tube: 3/8 inch i.d. and 1/2 inch o.d.) packed with magnesium perchlorate and Ascarite II (Fisher) to ensure the complete removal of water moisture and CO_2. The N_2 "gas divider" is a Valco tee (1/16 inch tubing o.d.) with a changeable fused silica tube outlet (0.32 mm i.d.). The dividing ratio is 95 / 5, releasing 95 % of the gas stream out of the system during transport. The dividing ratio can be adjusted by changing the flow rate of the fused silica tube outlet (O3). The N_2O and N_2 traps were made of a U-shaped stainless steel tube (40 cm long 1/16 inch o.d. and 0.04 inch i.d.) respectively filled with nickel wires and the other with a molecular 5Å sieve (60/80 granular, GRACE). In our system, N_2O bypasses the copper furnace; that is, N_2O is measured nondestructively to avoid the bias caused by incomplete reduction reaction (N_2O or NO to N_2). The standard gas we used for calibration is a mixture of N_2 and N_2O (2000 and 100 ppm, respectively). In the preparation system, the sample gas flows through the fused silica tube (430 µm o.d., 320 µm i.d.), while the

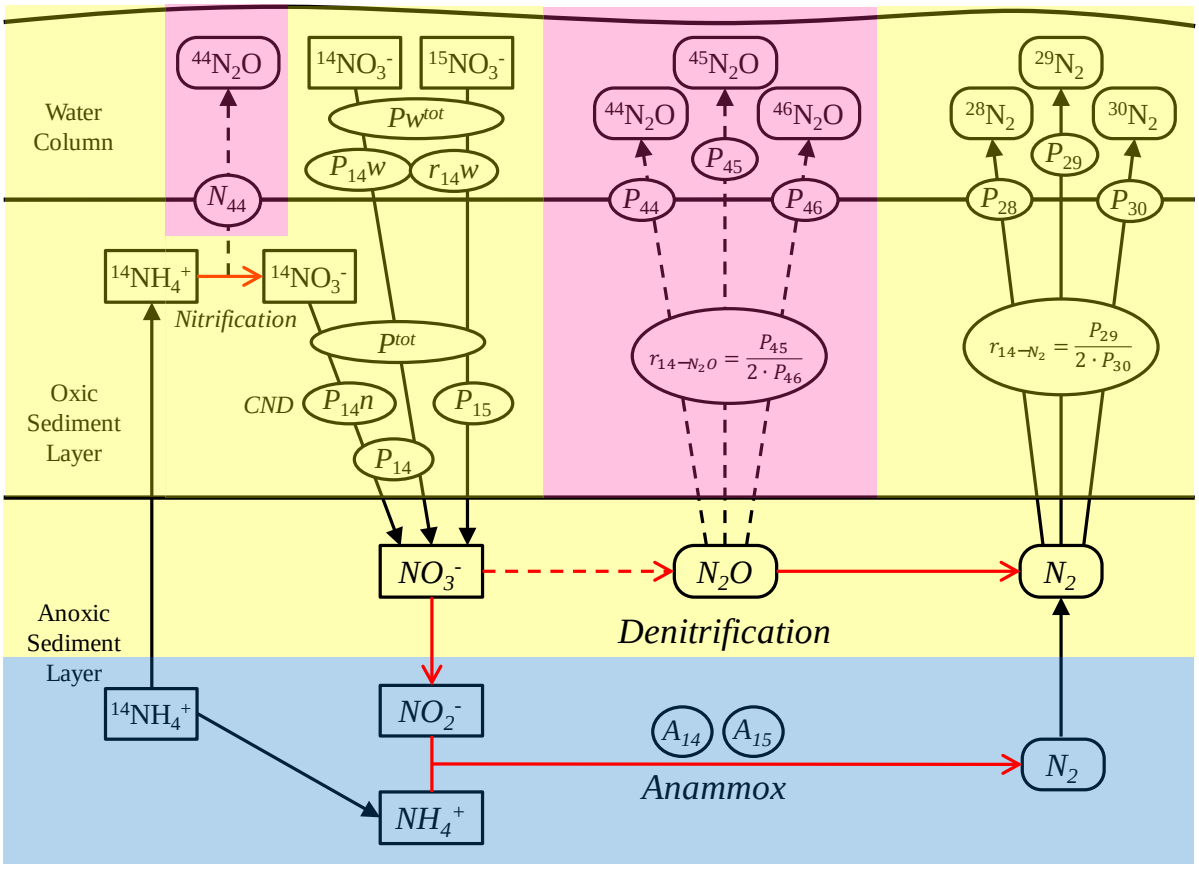

Fig. 1. Schematic diagram of various N transformation processes and rates considered by different versions of IPT (after ref. 11). Yellow plate represents $IPT_{classic}$. Yellow and blue plates represent IPT_{ana}. Yellow and pink plates represent IPT_{N_2O}. The full diagram represents IPT_{anaN_2O}. Gases isotopic N_2 and/or N_2O production rates in individual process are designated, respectively, as "P_x" or "A_x" (e.g., P_{14} or A_{14}). Detailed explanation of the abbreviations is given in Table 1. The equations of r_{14-N_2} and r_{14-N_2O} represent the ratio between using $^{14}NO_3^-$ and $^{15}NO_3^-$ during nitrate reduction in different estimators. CND is the process of coupled nitrification–denitrification.

standard and carrier gases flow through the stainless steel tube (1/16 inch o.d.; 0.04 inch i.d.).

The analytical procedure includes three phases: sample loading, N_2 injection and N_2O injection. In sample loading phase, helium gas (99.999 % purity) bubbles gases out of the vial to the sample preparation line. A complete extraction of N_2 and N_2O would take 5 min at a flow rate of 21 mL min^{-1} (O3 + O5). The gas sample flows through the chemical column while V1 is at the "sample" position (Fig. 2). After flowing through the Nafion tube membrane, the gas sample flows into the two cryogenic traps. N_2O is captured, concentrated and retained when the first trap is submerged in liquid nitrogen (LN_2). The trapping efficiency of N_2O is better than 95 %, as validated using the standard gas. N_2 is trapped in the second trap assembled on V3. In between the two traps a copper oxidation furnace fixed at 600 °C was installed to remove O_2 from the flowing stream and to convert trace NO_x into N_2. The gas divider allows 5 % of the target gas to be trapped, thus ensuring that N_2 would not exceed the detection range of the IRMS.

In the N_2 injection phase, the N_2 trap was pulled up and heated to 300 °C within 20 s to release the captured N_2. At the same time, V3 was switched to "injection" mode to allow for helium gas (at a flow rate of 2 mL min^{-1} for 3 min) to flush N_2 through the GC column and the Nafion membrane and then into the IRMS. After the N_2 injection phase was completed, the N_2O trap was elevated above LN_2, and V2 and V3 were then respectively switched to the "injection" and "loading" positions for 7 min at room temperature to release N_2O. Meanwhile, the preparation line was backflushed for cleaning by two helium gas streams mounted on V2.

However, in studies on highly enriched ^{15}N tracers, the target gases frequently give signals that exceed the normal range of IRMS detectors. In addition to the original resistors on the amplifiers (3×10^8, 3×10^{10} and 1×10^{11} Ω), we added a second set of resistors 3×10^{10}, 3×10^8 and

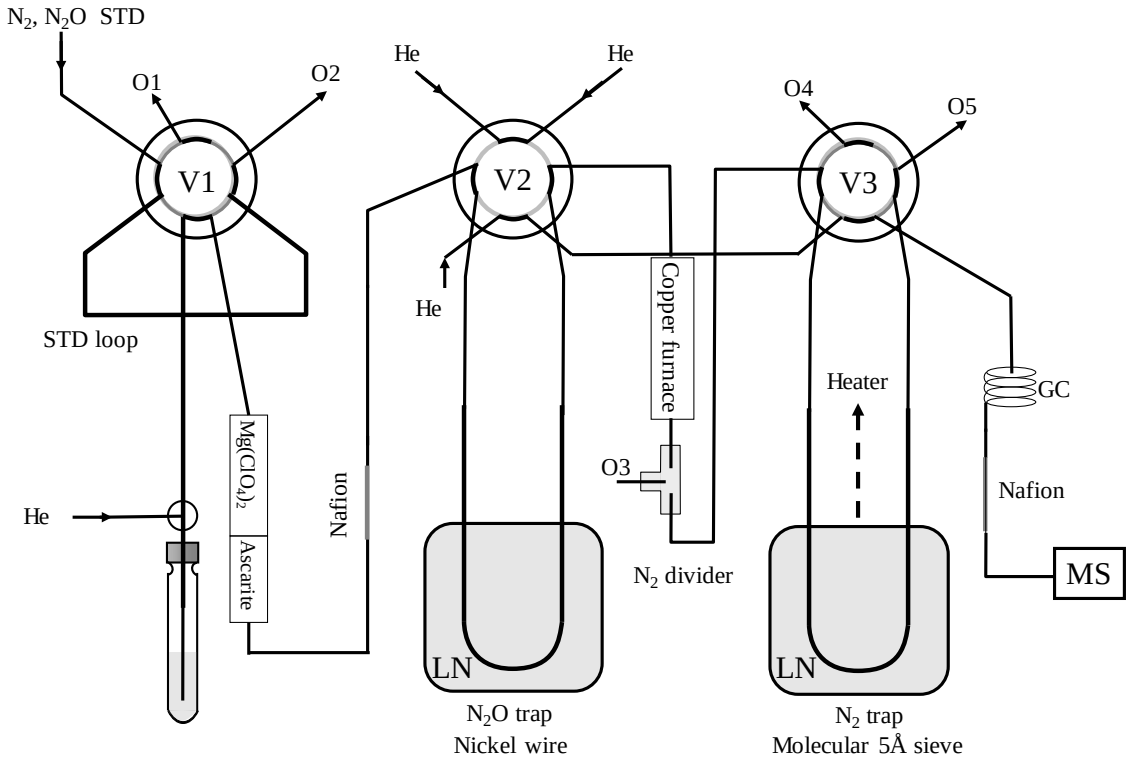

Fig. 2. Schematic diagram of preconcentration system at sample loading phase: GC, gas chromatogram column (ConFlow); He, helium; LN, liquid nitrogen; MS, mass spectrometer; O1–5, outlets to atmosphere; STD, standard gas; and V1–3, automated control valves. Please refer to text for details.

$3 \times 10^8\ \Omega$ to cups 1, 2 and 3, respectively. Combining the N_2 divider with the second set of resistors in the IRMS made it possible to detect a wide range of ^{15}N tracers. The overall design obtained the signal of m/z 44, which represents the absolute amount of N_2O. After proper calibration using standard gases, this signal can be applied to IPT calculations.

2.2 Validation of instrument modifications

The reproducibility and linearity of IRMS signals are critical to obtaining accurate results. In our system, the most significant instrument modification is the inclusion of the two additional cryogenic sample traps and the gas divider. We applied three kinds of test for verification. Different volumes of standard gas (mixture of N_2 and N_2O) were used for calibration by varying the length of the STD loop (Fig. 2). The linear responses ($r^2 = 1$ for all) were shown in signal areas of m/z 28, 29 and 30 over a range from 2 to 32 µmol for N_2 and areas of m/z 44, 45 and 46 over a range from 4 to 83 nmol for N_2O (Fig. 3). The good signal reproducibility could be ascertained from the small relative standard deviation for N_2 (1.5 to 2.3 % for three isotopic species, $n = 70$) and for N_2O (below 1.5 % for three isotopic species, $n = 80$). Constant ratios for m/z 29/28, m/z 30/28, m/z 45/44 and m/z 46/44 were observed throughout the calibrations. Note that in Fig. 3a, a N_2 background signal (intercept 7.75 µmol in $^{28}N_2$) was observed; yet such a signal was expected and would affect neither the calculation of excess ^{15}N ratio (1992) nor the production of $^{29}N_2$ and $^{30}N_2$. The trap efficiency was further tested by injecting a given amount of standard gas mixture through the preparation line without trapping. These signals were compared with those under the operation of cryogenic traps. Results showed a high and stable trapping efficiency for N_2 and N_2O over a wide signal range (> 90 %). In the third batch validation, we used different volumes of water saturated with the standard gas mixture to check the signal recovery after the entire procedure had been completed. The results (not shown) are very good, showing consistent trap efficiencies and a stable dividing ratio of the gas divider throughout all measurements.

Meanwhile, we validated the reliability of the additional amplification factors by cross-checking signals provided by the two amplifiers of the same cup with a given amount of N_2 gas. The results of the three cups were consistent following signal conversion (t test, $p > 0.05$, $n = 15$). The conversion factor agreed perfectly with the expected amplification factor.

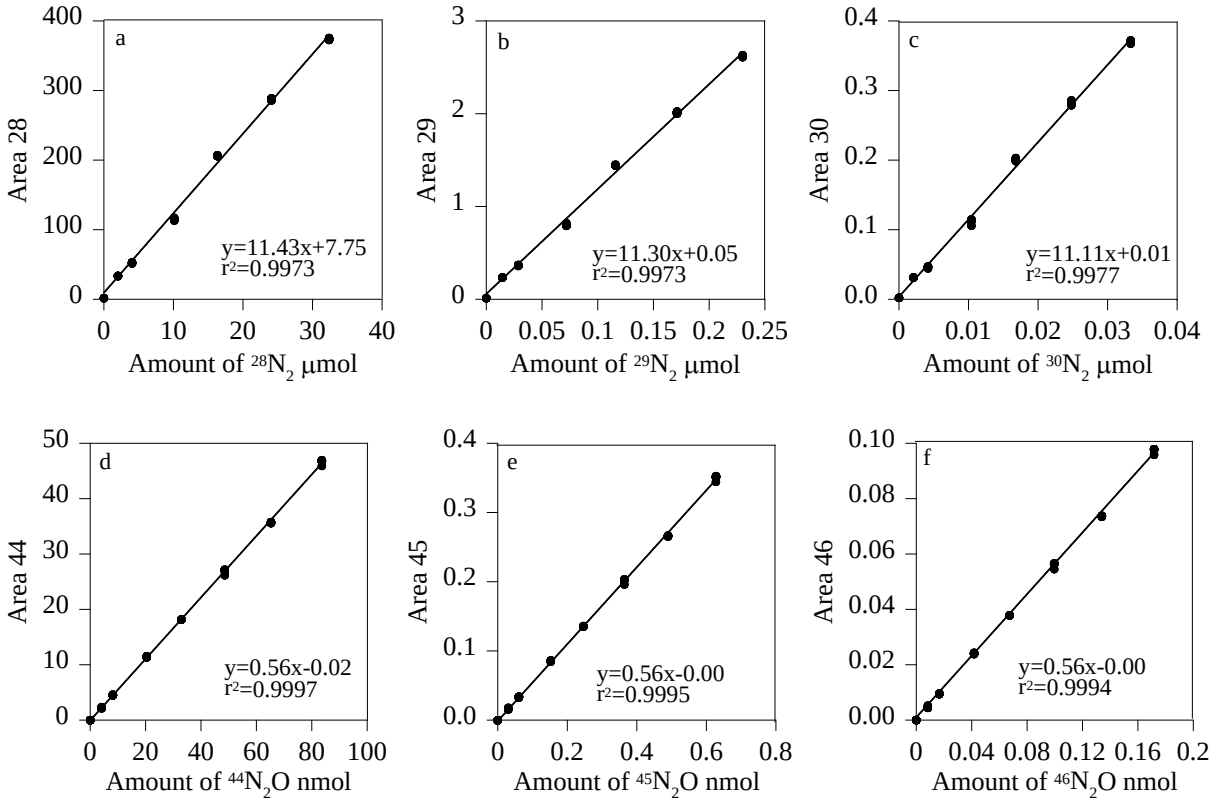

Fig. 3. (a, b, c) Linear responses of signal area m/z 28, 29 and 30 against given amounts of standard gas $^{28}N_2$, $^{29}N_2$ and $^{30}N_2$, respectively. **(d, e, f)** Linear responses of signal area m/z 44, 45 and 46 to various amounts of stand gas $^{44}N_2O$, $^{45}N_2O$ and $^{46}N_2O$, respectively.

3 Development of IPT

3.1 Reported IPT estimators

The critical parameter in IPT is r_{14} (Fig. 1), an estimation ratio between $^{14}NO_3^-$ and $^{15}NO_3^-$ undergoing denitrification in the nitrate reduction layer. In $IPT_{classic}$, as proposed by Nielsen (1992), r_{14} was derived from the production rates of $^{29}N_2$ (P_{29}) and $^{30}N_2$ (P_{30}) as

$$r_{14-N_2} = \frac{P_{29}}{2 \cdot P_{30}}. \quad (1)$$

There are three major assumptions behind the above equation: (1) production rates of isotopic nitrogen gases species obey the binomial distribution (i.e., $^{28}N_2$, $^{29}N_2$ and $^{30}N_2$ in $IPT_{classic}$; $^{44}N_2O$, $^{45}N_2O$ and $^{46}N_2O$ in other versions of IPT), (2) the ratio between $^{14}NO_3^-$ and $^{15}NO_3^-$ is constant in the NO_3^- reduction zone and (3) denitrification is the only pathway for N_2 production (see Sect. 4.3 for detail). Thus, the isotope composition of N_2 should reflect that of the reduced NO_3^-. The genuine N_2 production from denitrification ($P_{14-classic}$ or $D_{14-classic}$, see Fig. 1) is estimated as

$$P_{14-classic} = D_{14-classic} = r_{14-N_2} \cdot (2 \cdot P_{30} + P_{29}), \quad (2)$$

where the suffix N_2 denotes parameters derived solely from $^{15}N_2$ production rates.

Similar to denitrification, anammox also produces N_2, yet the two atoms of N in N_2 from anammox are sourced from NH_4^+-N and NO_2^--N in a 1 : 1 mole ratio (van de Graaf et al., 1997). This recently discovered nitrogen removal process (Mulder et al., 1995) was of course not included in the $IPT_{classic}$ when it was proposed. The presence of anammox violates the basic assumptions of $IPT_{classic}$ and causes overestimation in $D_{14-classic}$, which was clearly explained by Risgaard-Petersen et al. (2003). Accordingly, a revised version of IPT (IPT_{ana}) was recommended to properly estimate the genuine N_2 production (P_{14-ana}) from anammox and denitrification in sediments (Risgaard-Petersen et al., 2003).

Similar to $IPT_{classic}$, the IPT_{ana} method was used to conduct ^{15}N nitrate enrichment in intact sediment core incubations and direct measurement of P_{29} and P_{30}. However, Risgaard-Petersen et al. (2003) introduced two indirect approaches to derive r_{14}. The first approach requires additional slurry incubation by adding $^{15}NH_4^+$ to measure the proportional contribution of anammox to total N_2 production (*ra*). The second approach requires additional sets of sediment core incubation to generate a linear relationship of $^{15}N_2$ production rates against $^{15}NO_3^-$ enrichment gradients to indirectly eliminate anammox-biased r_{14}.

Trimmer et al. (2006) suggested using $^{15}N_2O$ to derive r_{14} (r_{14-N_2O}) to avoid the bias from anammox. When anammox

exists, P_{29} (Fig. 1) is contributed partially from anammox ($^{14}NH_4^+ + {}^{15}NO_2^-$), and thus r_{14-N_2} is unsuitable to represent the $^{14}N/{}^{15}N$ ratio of NO_3^- reduced by denitrifiers. Since $^{15}N_2O$ was only sourced from denitrification, the r_{14-N_2O} is more representative and is no longer influenced by anammox (Trimmer et al., 2006). Similarly, the distribution of $^{15}N_2O$ isotopic species will follow the fundamental assumptions of $IPT_{classic}$ regarding the distribution of $^{15}N_2$ isotopic species and can be used to estimate r_{14} as

$$r_{14-N_2O} = \frac{P_{45}}{2 \cdot P_{46}}, \tag{3}$$

where P_{45} and P_{46} are the production rates of $^{45}N_2O$ and $^{46}N_2O$, respectively. According to Risgaard-Petersen et al. (2003) the genuine N_2 production (P_{14-ana}) can be expressed as

$$P_{14-ana} = D'_{14-N_2} + A_{14}, \tag{4}$$

where D'_{14-N_2} and A_{14} respectively represent the genuine N_2 production from denitrification and anammox (Fig. 1). Accordingly, D'_{14-N_2} and A_{14} can be expressed in terms of measurable parameters, r_{14-N_2O}, P_{29} and P_{30}:

$$D'_{14-N_2} = \left(r_{14-N_2O} + 1\right) \cdot 2 \cdot r_{14-N_2O} \cdot P_{30} \tag{5}$$

and

$$A_{14} = 2 \cdot r_{14,\,N_2O} \cdot \left(P_{29} - 2 \cdot r_{14-N_2O} \cdot P_{30}\right), \tag{6}$$

where the formula $P_{29} - 2 \cdot r_{14-N_2O} \cdot P_{30}$ represents the anammox N_2 production by utilizing $^{15}NO_3^-$ (A_{15}). Substituting Eq. (4) with Eq. (5) and Eq. (6), P_{14-ana} becomes

$$P_{14-ana} = 2 \cdot r_{14,\,N_2O} \cdot \left[P_{29} + P_{30} \cdot \left(1 - r_{14-N_2O}\right)\right]. \tag{7}$$

However, based on Neilsen's $IPT_{classic}$ (1992), Master et al. (2005) proposed that IPT_{N_2O} ought to include the rate of N_2O production in the total denitrification rate; nevertheless, they ignored anammox (Fig. 1). According to their assumption, denitrification is the only NO_3^- reduction process to be considered in IPT_{N_2O}, and thus the distribution of $^{15}N_2$ and $^{15}N_2O$ isotopic species should be equal and is expressed as

$$r_{14-N_2} = r_{14-N_2O}. \tag{8}$$

Thus, IPT_{N_2O} estimates the genuine N_2 and N_2O production from denitrification (D_{14-N_2} and D_{14-N_2O}, respectively, see Fig. 1) by the following equation:

$$\begin{aligned} P_{14-N_2O} &= D_{14-N_2} + D_{14-N_2O} \\ &= r_{14-N_2O} \cdot (2 \cdot P_{30} + P_{29}) \\ &\quad + r_{14-N_2O} \cdot (2 \cdot P_{46} + P_{45}) \\ &= r_{14-N_2O} \cdot (2 \cdot P_{30} + P_{29} + 2 \cdot P_{46} + P_{45}). \end{aligned} \tag{9}$$

3.2 Modified IPT method

As mentioned earlier, previously reported IPT methods have various flaws. Given that both N_2 and N_2O can be precisely measured after incubation, we propose a modified IPT (IPT_{anaN_2O}) estimator, which integrates IPT_{ana} and IPT_{N_2O} into complete estimations of gaseous nitrogen production in ^{15}N nitrate-enriched experiments.

IPT_{anaN_2O} involves the production of (1) N_2 from denitrification, (2) N_2 from anammox, (3) N_2O from denitrification and (4) N_2O from nitrification, thus representing a combination of IPT_{ana} and IPT_{N_2O} as shown in Fig. 1. The parameters D'_{14-N_2}, A_{14} and D_{14-N_2O} in the proceeding equations can be derived independently. Therefore, the accurate total genuine N_2 and N_2O production ($P_{14-anaN_2O}$) from all related processes can be summarized as

$$\begin{aligned} P_{14-anaN_2O} &= D'_{14-N_2} + A_{14} + D_{14-N_2O} \\ &= \left(r_{14-N_2O} + 1\right) \cdot 2 \cdot r_{14-N_2O} \cdot P_{30} \\ &\quad + 2 \cdot r_{14-N_2O} \cdot \left(P_{29} - 2 \cdot r_{14-N_2O} \cdot P_{30}\right) \\ &\quad + r_{14-N_2O} \cdot (2 \cdot P_{46} + P_{45}) \\ &= 2 \cdot r_{14-N_2O} \cdot \left[P_{29} + P_{30}\left(1 - r_{14-N_2O}\right)\right] \\ &\quad + r_{14-N_2O} \cdot (2 \cdot P_{46} + P_{45}). \end{aligned} \tag{10}$$

Similar to Risgaard-Petersen et al. (2003) the $P_{14-anaN_2O}$ can be further separated into two components – (1) genuine N_2 and N_2O production supported by water-column-delivered nitrate ($P_{14}w$), and (2) genuine N_2 and N_2O production supported by coupled nitrification–denitrification ($P_{14}n$):

$$P_{14}w = P_{14-anaN_2O} \cdot \frac{r_{14}w}{r_{14-N_2O}} \tag{11}$$

$$\begin{aligned} P_{14}n &= P_{14-anaN_2O} - P_{14}w \\ &= P_{14-anaN_2O} \cdot \left(1 - \frac{r_{14}w}{r_{14-N_2O}}\right), \end{aligned} \tag{12}$$

where $r_{14}w$ is the ratio of $^{14}NO_3^-$ to $^{15}NO_3^-$ in the water column. Equations (11) and (12) should be used carefully, and arguments associated with the concept of nitrate sources for denitrification were discussed in Middelburg et al. (1996a, b) and Nielsen et al. (1996). In the model simulation, separating nitrate sources into bottom-water-supported and nitrification-coupled components is only correct in an uncoupled system (Fig. 1) where nitrification and denitrification occur in distinct zones (Middelburg et al., 1996a). However, the model results also suggested that separation of nitrate sources is not physically real because of the spatial overlap of nitrification and denitrification and different diffusion gradient between $^{14}NO_3^-$ and $^{15}NO_3^-$.

We can also obtain another crucial parameter, *ra*, which can be used to separate the fractional contribution of N_2 from that of anammox. According to Risgaard-Petersen et

al. (2003), *ra* is expressed as

$$ra = \frac{A_{14}}{D'_{14-N_2} + A_{14}}. \quad (13)$$

Trimmer et al. (2006) suggested an alternative approach to derive *ra* after completing $^{15}NO_3^-$ concentration series experiments (see below). According to Trimmer et al. (2006), the term r_{14} is converted into another parameter,

$$q = \frac{1}{r_{14} + 1}, \quad (14)$$

where q is the proportion of ^{15}N in the NO_3^- pool undergoing denitrification. Since r_{14} can be derived from $^{15}N_2$ or $^{15}N_2O$, the qN_2 is directly related to r_{14-N_2} and the qN_2O is related to r_{14-N_2O}. By regression analysis, the slope of the qN_2 against qN_2O derived from $^{15}NO_3^-$ concentration series incubations can form an equation for *ra*:

$$ra = \frac{2 - 2 \cdot \text{slope}}{2 - \text{slope}}. \quad (15)$$

Note that, mathematically, the value of *ra* derived from Eq. (13) is equal to that derived from Eq. (15), though it may appear that the two equations might have been misled by different methods (see Appendix A). However, the benefit of Eq. (15) is that through $^{15}NO_3^-$ concentration series incubations we can directly derive the average *ra* from the plot of the qN_2 vs. qN_2O (e.g., Fig. 5).

Master et al. (2005) described how N_2O produced by nitrification can be derived by calculation. Theoretically, the $^{44}N_2O$ directly measured by IRMS ($[D_{44} + N_{44}]_{IRMS}$) consists of two components – the $^{44}N_2O$ formation via nitrification (N_{44}) and denitrification (D_{44}). Accordingly, N_{44} can be expressed as

$$N_{44} = [D_{44} + N_{44}]_{IRMS} - D_{44}, \quad (16)$$

where D_{44} is calculated from

$$D_{44} = P_{45} \cdot \frac{r_{14-N_2O}}{2}. \quad (17)$$

All the parameters mentioned above are listed in Fig. 1 and defined in Table 1. Now we have all the parameters needed to separate the production of N_2 and N_2O from different processes.

Similarly, IPT_{anaN_2O} inherited a series of assumptions in $IPT_{classic}$, IPT_{ana} and IPT_{N_2O}. Below we list all assumptions and explain how we evaluate their validity.

1. A steady-state nitrate concentration profile across the sediment–water interface must be established shortly after the addition of $^{15}NO_3^-$.

2. The parameter r_{14} (i.e., the ratio of $^{15}NO_3^-$ to $^{14}NO_3^-$ undergoing denitrification) remains constant in the nitrate reduction zone, resulting in an ideal binomial distribution of the formed N_2O species.

3. Denitrification is the only quantitatively significant source of $^{15}N_2O$, and is limited by the supply of NO_3^- from the overlying water.

4. Anammox is limited by NO_3^- during the $^{15}NO_3^-$ labeling experiment.

5. The mole fraction of ^{15}N in the NO_3^- and NO_2^- pools undergoing dissimilatory reduction is equal.

6. Nitrification is not affected by the addition of $^{15}NO_3^-$.

Except for assumptions 5 and 6, all of the above assumptions can be evaluated via the response of $^{15}N_2O$ and $^{15}N_2$ in the three types of incubations discussed in Sect. 4.3.

A field experiment was also conducted to evaluate the applicability of our modified method and test the validity of the above assumptions.

4 Field experiment and assessment of IPT estimators

4.1 Sampling site and experiment design

In June 2011, sediment samples were collected at low tide from the intertidal zone of the Danshuei River (25°06′38.37″ N, 121°27′52.10″ E), northern Taiwan's largest river. The sediments are fine with a porosity of 0.76 (v/v) and moderate organic carbon content (2.3 % dry weight). Nitrate and ammonium concentrations in the overlying water were about 30 and 180 µM, respectively. At the time of collection the water temperature was ∼ 26 °C, similar to the air temperature. A total of 36 sediment cores were collected using Plexiglas tubes (30 cm long, 4.5 cm i.d.). An additional 500 g of surface sediments (top 1 cm) were taken and stored in plastic bags for slurry incubation. The sediments were returned to the lab within two hours of collection. Overlying water in the sediment cores was adjusted to 7 cm by carefully removing the bottom sediments. The intact sediment cores were then equilibrated with oxygen saturated river water at 26 °C in a tank overnight. Three types of incubations were performed following Trimmer et al. (2006).

In the $^{15}NO_3^-$ concentration series experiment, we added $^{15}NO_3^-$ (100 mM, 98 % ^{15}N atom; Sigma-Aldrich) with final concentrations of 50, 100, 150 and 200 µM in the overlying water and a total of six replicates for each concentration. All cores were sealed, with overlying water stirred by a small stir bar (located at the top 4 cm) below the surface of the overlying water driven by a large external magnet (with the incubation tank following the design by Trimmer et al. (2006)). To ensure a constant ratio between $^{14}NO_3^-$ and $^{15}NO_3^-$ in the nitrate reduction layer, a preincubation time of 30 min was adopted. Three replicates were sacrificed from each treatment immediately at time zero (t_0), while the remaining three replicates were sacrificed after every 3 h of incubation at 26 °C, close to in situ temperature.

Table 1. List of abbreviations used in equations.

Abbreviations	Definitions
P_{29}	Production rate of $^{29}N_2$ determined with excess ^{15}N ratio
P_{30}	Production rate of $^{30}N_2$ determined with excess ^{15}N ratio
P_{45}	Production rate of $^{45}N_2O$ determined with excess ^{15}N ratio
P_{46}	Production rate of $^{46}N_2O$ determined with excess ^{15}N ratio
$[D_{44} + N_{44}]_{IRMS}$	Production rate of $^{44}N_2O$ calculated as signal area (concentration) change of m/z 44 over time
r_{14}	Ratio between $^{14}NO_3^-$ and $^{15}NO_3^-$ undergoing nitrate reduction
r_{14-N_2}	Estimator of r_{14}, based on $^{15}N_2$ production
r_{14-N_2O}	Estimator of r_{14}, based on $^{15}N_2O$ production
$r_{14}w$	Ratio between $^{14}NO_3^-$ and $^{15}NO_3^-$ in the water column
q	Fraction of ^{15}N in NO_3^- pool undergoing reduction
qN_2	Estimator of q, based on $^{15}N_2$ production
qN_2O	Estimator of q, based on $^{15}N_2O$ production
$D_{14-classic}$	Denitrification N_2 production rate by reactions using $^{14}NO_3^-$ as substrate estimated with $IPT_{classic}$
D_{14-N_2}	Denitrification N_2 production rate by reactions using $^{14}NO_3^-$ as substrate estimated with IPT_{N_2O}
D'_{14-N_2}	Denitrification N_2 production rate by reactions using $^{14}NO_3^-$ as substrate excluding anammox
D_{14-N_2O}	Denitrification N_2O production rate by reactions using $^{14}NO_3^-$ as substrate
D_{44}	$^{44}N_2O$ production rate via denitrification
A_{14}	Anammox N_2 production rate supported with $^{14}NO_3^-$
A_{15}	Anammox N_2 production rate supported with $^{15}NO_3^-$
$P_{14-classic}$	Genuine N_2 production rate estimated with $IPT_{classic}$, equal to $D_{14-classic}$
P_{14-ana}	Genuine N_2 production rate estimated with IPT_{ana}
P_{14-N_2O}	Genuine N_2 and N_2O production rate estimated with IPT_{N_2O}
$P_{14-anaN_2O}$	Genuine N_2 and N_2O production rate estimated with IPT_{anaN_2O}
$P_{14}w$	Genuine N_2 and N_2O production rate supported by the nitrates from water column
$P_{14}n$	Genuine N_2 and N_2O production rate supported via coupled nitrification
ra	Contribution of anammox to N_2 production
$ra_{(N_2+N_2O)}$	Contribution of anammox to N_2 and N_2O production
N_{44}	Production rate of N_2O via nitrification

The remaining 12 sediment cores were used for $^{15}NO_3^-$ time series experiments, in which all overlying waters were enriched to 50 µM of $^{15}NO_3^-$. We sacrificed three samples as replicates at 1 h intervals over three hours, starting from time zero (t_0, t_1, t_2 and t_3).

To subsample the sediment cores of the two above-mentioned experiments, we followed the protocol established in Dalsgaard et al. (2000) by mixing the overlying water and approximately the top 1 cm of sediments gently with a glass rod. A total of 4 mL of mixed slurry was filled into a gas-tight vial (Exetainer, 12 mL) containing 100 µL of formaldehyde solution (38 % w/v) and a glass bead (5 mm diameter) for mixing. After capping, the headspace was quickly flushed with helium to remove unwanted air. The entire process took a maximum of 2 min to finish. The production rates of $^{29}N_2$, $^{30}N_2$, $^{45}N_2O$ and $^{46}N_2O$ were calculated as the excess ^{15}N ratio (Nielsen, 1992).

The potential activities of denitrification and anammox were measured. Following Risgaard-Petersen et al. (2004), but with slight modifications, we mixed ~ 100 mL of surface sediment with 100 mL of filtered (0.2 µm) river water in a beaker, and then bubbled with helium gas to remove oxygen. Anaerobic conditions were confirmed by the oxygen microsensor (Unisense SA). A total of 36 slurry samples were prepared by transferring 4 mL of slurry to each gas-tight vial (Exetainer, 12 mL) and immediately purged with helium gas to ensure they were oxygen-free after being capped. All vials were preincubated overnight to allow for the complete consumption of NO_3^-, NO_2^- ($^{14}NO_x^-$) and O_2. (Additional measurements confirmed that NO_x^- was consumed completely after preincubation). The slurries were then enriched with (1) $^{15}NH_4^+$ (the concentrated stock of 100 mM, 98 ^{15}N atom %; Sigma-Aldrich), (2) $^{15}NO_3^-$ and (3) $^{15}NH_4^+$ versus $^{14}NO_3^-$ to a final concentration of 100 µM (wet slurry). The incubations were stopped at 1 h intervals over a 3 h period by injecting 0.1 mL of formaldehyde.

4.2 Evaluation of different versions of IPT

Figure 4 presents the experimental results. We compared N_2 and N_2O production rates derived from various IPT methods. IPT_{anaN_2O} resulted in a N_2 production rate (D'_{14-N_2}) of 42.3 ± 6.4 µmol N m^{-2} h^{-1}, which was equal to that derived from IPT_{ana}. Both IPT versions applied r_{14-N_2O} with

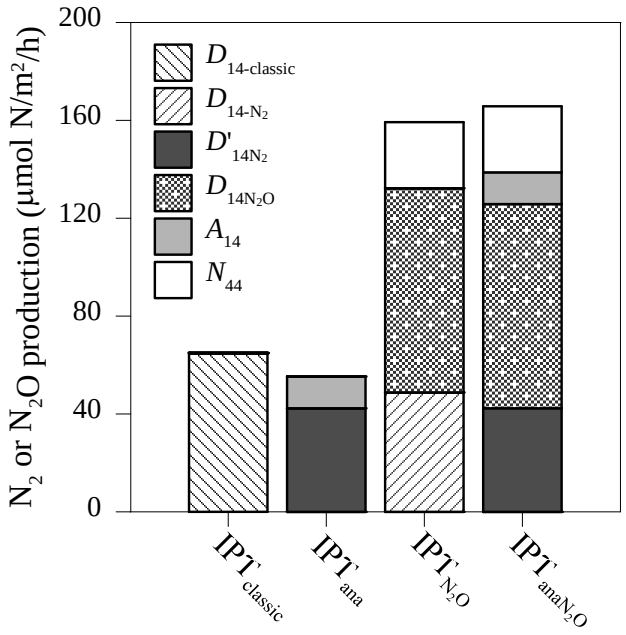

Fig. 4. Comparison of N_2 or N_2O production rates estimated by different versions of IPT.

consideration of anammox in their calculations. However, using $IPT_{classic}$ and IPT_{N_2O} can result in overestimating the denitrification rate. In $IPT_{classic}$, the denitrification rate, $P_{14-classic}$ ($D_{14-classic}$), was $64.9 \pm 11.2\,\mu mol\,N\,m^{-2}\,h^{-1}$, which is apparently biased due to improper r_{14-N_2} and ignoring anammox. When the r_{14-N_2O} was applied to IPT_{N_2O}, the N_2 production (D_{14-N_2}) was $48.8 \pm 7.7\,\mu mol\,N\,m^{-2}\,h^{-1}$, which was still an overestimate because anammox was neglected. Thus, IPT_{ana} and IPT_{anaN_2O} conclusively provide the most appropriate estimation in consideration of the sole end product of N_2 from the complete denitrification.

N_2O from incomplete denitrification has to be taken into account in estimating the total denitrification rate, which is accomplished using IPT_{N_2O} and IPT_{anaN_2O}. Both methods gave the same N_2O production rates (D_{14-N_2O}) of $83.4 \pm 11.8\,\mu mol\,N\,m^{-2}\,h^{-1}$, which is two times the D'_{14-N_2}. The N_2O yield (production rates of N_2O relative to the total denitrification; defined as $D_{14-N_2O}/D_{14-N_2O}+D'_{14-N_2}$)) was 66 % by IPT_{anaN_2O}. This proportion is not low at all and should not be overlooked. Although N_2O yields ($N_2O/(N_2+N_2O)$) via denitrification were reported to be < 2 % in many previous studies, some other cases recorded high N_2O yield in estuarine sediments. For example, Dong et al. (2002) observed N_2O yields from 0 to ~ 9 %, with one exceptionally high yield (~ 50 %) in the Colne Estuary. They concluded that NO_2^- is favored as a denitrifier to form N_2O and may be a critical factor regulating the formation of N_2O. In other British rivers and estuaries, a wide range of N_2O yield (0 to 100 %) has also been observed (García-Ruiz et al., 1998a; García-Ruiz et al., 1998b). The causes for such high N_2O yield were not well explored; however, our high yield might not be out of the ordinary. Note that the yield number in our study remains constant throughout four concentrations in the $^{15}NO_3^-$ addition experiment (slope = 0.0, $p > 0.05$), indicating that the effect of $^{15}NO_3^-$ enrichment was negligible and a homogenous incubation environment was achieved in the sediment cores. Minjeaud et al. (2008) performed field tests for IPT_{N_2O} in a coastal lagoon. In contrast to our results, they reported a dramatic increase of N_2O yields from 0 to 75 % as they increased the $^{15}NO_3^-$ concentrations. They speculated that the analytical procedure of the isotopic composition of N_2O was insufficiently sensitive in the presence of low nitrate concentrations. In our study, the nitrate concentrations were an order of magnitude higher than those in their study sites. Dong et al. (2006) used IPT_{N_2O} for estuary sediments, but did not test the response of N_2O yields with respect to different concentrations of added $^{15}NO_3^-$. More studies are needed to reconfirm the stable responses of N_2O yield in various environments.

N_2O contributed from unlabeled sources (N_{44}) and labeled sources (D_{14-N_2O}) can both be quantified by IPT_{anaN_2O}, providing important information for the understanding of the regulation factors of N_2O emissions. The total production rate of N_2O ($N_{44}+D_{14-N_2O}$) was $110\,\mu mol\,N\,m^{-2}\,h^{-1}$ in our field example. During sampling we also measured the in situ N_2O flux across the air–water interface as $72\,\mu mol\,N\,m^{-2}\,h^{-1}$. This flux was quantified by the independent method of Liss and Slater (1974). The IPT_{anaN_2O}-derived N_2O production rate is higher but within the same order of magnitude as the air–water N_2O flux. This difference may be due to two causes. First, the river water carried the signal from upstream, where the N_2O production rate is lower. Second, the N_2O produced in sediments might eventually be reduced to N_2 during diffusion in sediments, and thus the $N_{44}+D_{14-N_2O}$ falls between the gross and the net N_2O production during short incubation periods. Nevertheless, this result implies that most of the N_2O produced in the sediment of the Danshuei Estuary might eventually be released into the atmosphere.

The IPT_{anaN_2O} derived the genuine production rate of N_2 from anammox as $13.0 \pm 2.7\,\mu mol\,N\,m^{-2}\,h^{-1}$. This amount of N_2 accounts for 23 ± 4% of the genuine N_2 production (i.e., $ra = 0.23$; Fig. 5). Originally, *ra* was defined as the contribution of anammox to the total N_2 production to describe the contribution of anammox in nitrate removal processes. However, in environments with high N_2O yields, such as the Danshuei Estuary, D_{14-N_2O} should be included to better represent the relative net contribution of anammox. When the equation $ra_{(N_2+N_2O)} = A_{14}/P_{14-anaN_2O}$ is applied, the ratio is reduced to 12 %. Nevertheless, our modified method is more applicable to various environments such as lakes, rivers and coastal seas that have been reported as active sites of N_2O production (Bange et al., 1996; Seitzinger and

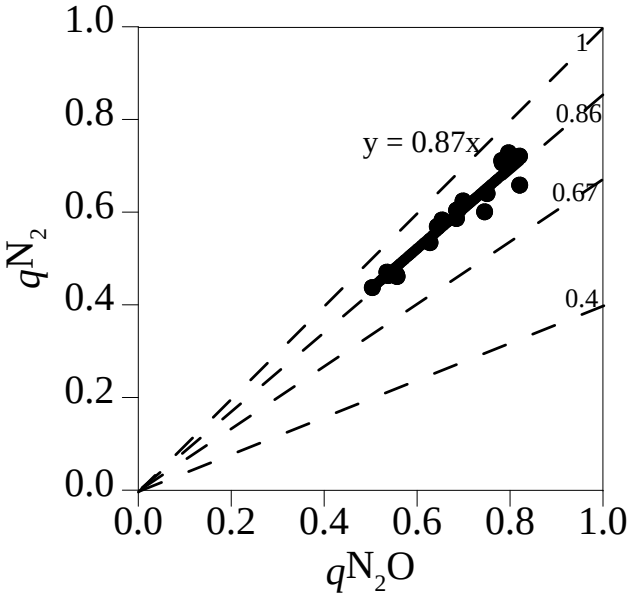

Fig. 5. The plot of qN_2 vs. qN_2O from concentration series incubations. Dashed lines represent the theoretical slope of 1, 0.86, 0.67 and 0.40, which corresponding to *ra* of 0, 25, 50 and 75 %, respectively. The slope of regression is 0.87 ± 0.03 ($r^2 = 0.95$, $p < 0.05$, $n = 21$) corresponding to *ra* of 23 ± 4 %.

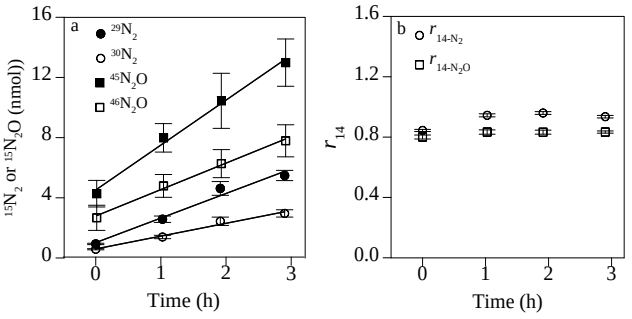

Fig. 6. Results from time series experiment. **(a)** Production of $^{15}N_2$ and $^{15}N_2O$ as a function of time. Regression coefficients (r^2) are 0.97, 0.98, 0.99 and 0.99 for $^{29}N_2$, $^{30}N_2$, $^{45}N_2O$ and $^{46}N_2O$, respectively. **(b)** Observational r_{14-N_2} and r_{14-N_2O} values as a function of time. Values are means ± 1 SEM ($n = 3$).

Kroeze, 1998) and widespread occurrence of anammox (Devol, 2008).

4.3 Validating the assumptions of our modified IPT_{anaN_2O}

Assumptions 1 and 2 describe a continuous and stable source of nitrate from overlying water for sedimentary denitrification and anammox. If the formation of N_2O follows the binomial distribution as stated in assumption 2, r_{14-N_2O} will be an appropriate proxy referring to the constant ratio of $^{14}NO_3^-$ and $^{15}NO_3^-$ (i.e., r_{14}). In our study, the linear increase of ^{15}N-labeled N_2 and N_2O concentrations in time series experiments indicated the appropriateness of the 3 h incubation time (Fig. 6a). Meanwhile, we found that the r_{14} value for N_2O and N_2 stayed constant during the incubation period (Fig. 6b). Moreover, in our $^{15}NO_3^-$ concentration series experiment, r_{14-N_2O} and r_{14-N_2} decreased as a function of the concentration of $^{15}NO_3^-$ added (Fig. 7a), and the maximum standard deviation was about 10 %, indicating a constant r_{14} for both gases throughout the incubation period. Also, the standard deviations of r_{14-N_2O} are smaller than that of r_{14-N_2}, implying r_{14-N_2O} is relatively stable. The above results indicated steady-state nitrate profiles were rebuilt both in the time series experiment and in the $^{15}NO_3^-$ concentration series experiment, thus satisfying the requirements of assumptions 1 and 2. Previous study has indicated that a similar experiment took only 8 min to reach equilibrium after adding the $^{15}NO_3^-$ tracer to the overlying water in intact sediment core incubation (Nielsen, 1992). Therefore, a 30 min preincubation procedure was recommended (Jensen et al., 1996; Lohse et al., 1996). However, in our experiment after preincubation, we still need one hour to reach the constant value of r_{14} for both gases. Apparently, our study environment required more time to reach equilibrium conditions. Note that the increment of r_{14-N_2O} from t_0 to t_1 was smaller than that of r_{14-N_2}, implying that r_{14-N_2O} reached a constant earlier than r_{14-N_2}. We speculated that the r_{14-N_2} response lag resulted from the relatively slow metabolic activity of anammox compared with denitrification (Strous et al., 1998).

Assumption 3, which involves $^{15}N_2O$ production, is critical in IPT_{ana}, IPT_{N_2O} and IPT_{anaN_2O} to accurately derive P_{14}. Mathematically we can resolve P_{14} by using the production of $^{15}N_2$ and $^{15}N_2O$ only if this assumption holds. Under this assumption, the "optimum" $P_{14} - P_{14-anaN_2O}$ – which considers both N_2O production and r_{14-N_2O}, can be derived by combining Eqs. (7) and (9). Since we do not consider the possible influence of other pathways – such as chemodenitrification, dissimilatory reduction of nitrate to ammonium (DNRA) and nitrifier denitrification (see below) – here we use the "optimum" for the current stage. A positive correlation between the production rate of $^{15}N_2O$ and the amount of $^{15}NO_3^-$ added (Fig. 7b) was observed in the $^{15}NO_3^-$ concentration series experiment indicating that denitrification is limited by NO_3^-. We also observed a relatively constant D_{14-N_2O} over various NO_3^- concentrations (Fig. 7c). Similar results were also revealed by P_{14-ana} and $P_{14-anaN_2O}$ in Fig. 7d. Those observations validated that in situ N_2O production via denitrification (D_{14-N_2O}) was not affected by the addition of $^{15}NO_3^-$ or by P_{14-ana} and $P_{14-anaN_2O}$. Also, this result implied that denitrification is the only quantitatively significant source of N_2O. By contrast, the dependency of $P_{14-classic}$ on the addition of $^{15}NO_3^-$ (Fig. 7c) would indicate an overestimation of $P_{14-classic}$. This overestimation is attributed to the second source of ^{14}N nitrogen, $^{14}NH_4^+$,

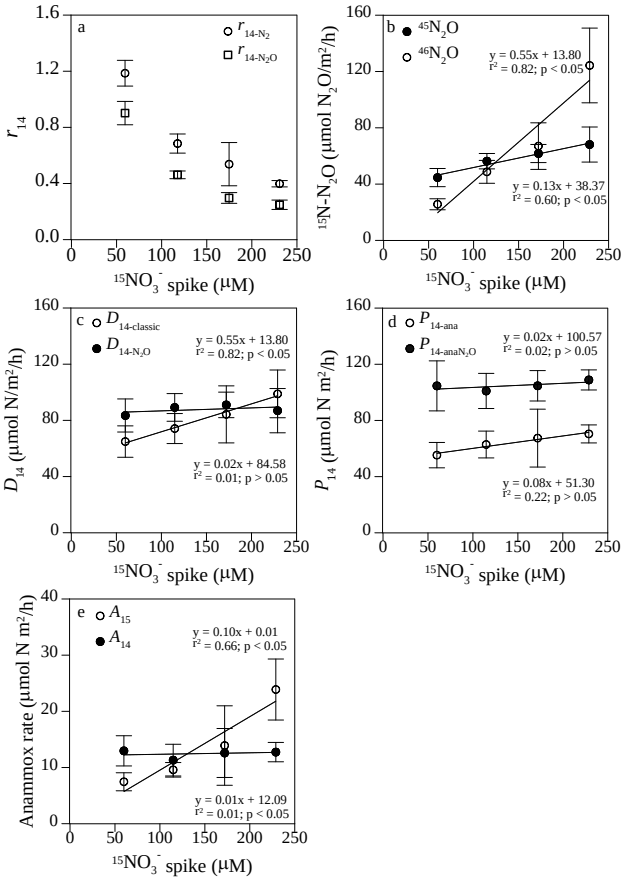

Fig. 7. Results from concentration series experiment. **(a)** r_{14} as a function of $^{15}NO_3^-$ spike, **(b)** production of $^{15}N_2O$ as a function of $^{15}NO_3^-$ spike, **(c)** comparison of denitrification N_2 production rates estimated by $IPT_{classic}$ ($D_{14-classic}$) and IPT_{N_2O} (D_{14-N_2O}), **(d)** comparison of genuine N_2 and N_2O production rates estimated by IPT_{ana} (P_{14-ana}) and IPT_{anaN_2O} ($P_{14-anaN_2O}$) and **(e)** the labeled (A_{15}) and unlabeled (A_{14}) anammox rates as a function of $^{15}NO_3^-$ spike. Values are means ±1 SEM ($n = 3$). Regression analysis used individual data ($n = 12$).

which was converted into a N_2 pool via the anammox process. However, the results from anoxic slurry incubations enriched with $^{15}NH_4^+$ showed no $^{15}N_2O$ signal to suggest the $^{15}N_2O$ from anammox is insignificant, although N_2O generated by anammox bacterial (pure strain) has been reported previously (Strous et al., 1998; van de Graaf et al., 1997). Meanwhile, our cross-checking experiment of the slurry incubations reconfirmed the occurrence of anammox, which potentially accounted for 20 % of the genuine N_2 production (data not shown).

Assumption 4 states that anammox is limited by NO_3^- as well as denitrification. We confirmed this assumption by the linear increase of A_{15} and the constant response of A_{14} during the addition of $^{15}NO_3^-$ (Fig. 7e). To our knowledge, this assumption has not been previously validated (e.g., Crowe et al., 2012; Trimmer and Nicholls, 2009). If the results do not support this assumption, anammox might be limited by NH_4^+. In this case, the *ra* and potential anammox activity could be estimated by slurry incubations enriched with $^{15}NH_4^+$ (Thamdrup and Dalsgaard, 2002).

Assumptions 5 and 6 are indispensable for all versions of IPT, but are difficult to verify specifically via IPT. Yet some inconsistent phenomena caused by the violation of these assumptions can be recognized, as illustrated by Risgaard-Petersen et al. (2003). Detailed descriptions are provided in Appendix B.

4.4 Uncounted nitrogen conversion pathways in IPT_{anaN_2O}

Nitrification and denitrification are assumed to be the only two processes to produce N_2O in IPT_{anaN_2O}. However, there are some other nitrogen conversion pathways that cannot be included in IPT_{anaN_2O}. For example, chemodenitrification, DNRA and nitrifier denitrification are potential N_2O producers in the field although almost all evidence in previous studies was obtained in the laboratory (Brandes et al., 2007; Wrage et al., 2001). Below we illustrated the potential inference of each individual pathway, if any.

Instead of measuring ^{15}N tracer signals, the N_{44} essentially relies on $^{44}N_2O$ formation measured by IRMS (see Eq. 16). If any uncounted N_2O-producing pathways from nondenitrification had occurred to an appreciable degree, the N_{44} will be more representative of the sum of N_2O production from nitrification and other uncounted pathways. Therefore, additional experiments, such as $^{15}NH_4^+$ enrichment, are needed to verify this parameter. In our field example, N_{44} was 27.0 ± 2.7 μmol N m^{-2} h^{-1}, and it might have been contributed by nitrification or, more precisely, "nondenitrification" pathways.

Chemodenitrification represents chemical reactions that lead to the conversion of NO_x^- or NH_4^+ to N_2O or N_2 (Davidson, 1992; Luther et al., 1997). This process usually prevails in extreme environments, such as those characterized by acidic or hydrothermal conditions (Brandes et al., 1998), and is presumably insignificant when compared with other microbial mediated processes. Once this process is shown to be prevalent in common aquatic environments, further revisions will be needed.

The observation of N_2O formation via DNRA has been proposed in pure cultures (Smith and Zimmerman, 1981; Smith, 1982). Again, due to methodological difficulties, no direct field evidence has shown that DNRA is a significant source of N_2O in sediment. The indirect field evidence revealed that DNRA might be a source of N_2O (Welsh et al. (2001) in an intertidal seagrass meadow. In the study of Welsh et al. (2001), parallel measurements of denitrification by the two techniques suggested that the denitrification rates measured by $IPT_{classic}$ (N_2 only) cannot explain the excess N_2O production in the acetylene-block technique. They

concluded that the excess N_2O was attributed to DNRA. However, one of possibilities was ignored in their paper – that the excess N_2O could be $^{15}N_2O$ from denitrification, which was the fraction they did not quantify in their $IPT_{classic}$ experiments.

Although some recent studies have found that DNRA is a significant source of NH_4^+ (Dong et al., 2011; Dong et al., 2009; Jäntti and Hietanen, 2012), we believe that the N_2O released via DNRA should be relatively insignificant in most environments. The favorable conditions for DNRA are strictly anaerobic sediments with a limited supply of NO_3^-. In such an environment, completely processing DNRA with the end product of NH_4^+ might be more efficient than the incomplete NO_3^- reduction that produces N_2O. Our idea is supported by Smith (1982), who observed a 90 % drop in N_2O production when NO_2^- changes from 15 000 to 150 µM in pure stain cultures. In addition, our slurry incubations showed that ^{15}N gas production accounted for a maximum 100 % of the added $^{15}NO_3^-$. This again suggested that DNRA is insignificant in our study site.

The metabolic processes of NO_3^- reducing to N_2O in denitrification and in DNRA have been demonstrated to be similar (Simon, 2002), and thus N_2O isotope composition may be indistinguishable between the two pathways by the $^{15}NO_3^-$ tracer approach. For this reason, r_{14-N_2O} should remain constant to reflect the $^{14/15}N$ ratio of the consumed NO_3^- even if DNRA is an alternatively significant source for N_2O. Therefore, rate estimations based on r_{14-N_2O} remain reliable in IPT_{anaN_2O}. If DNRA produces significant amounts of N_2O, the sole inference is the estimation of D_{14-N_2O}, which incorporates N_2O sourced from both denitrification and DNRA with no underestimate for nitrate removal rate.

Nitrifier denitrification has been demonstrated to be a N_2O-producing mechanism driven by versatile ammonia-oxidizing bacteria, *Nitrosomonas* spp. (Poth and Focht, 1985). The nitrifier involves three N_2O production pathways, namely ammonia oxidation (the first stage of nitrification,N_{44}), coupled nitrification–denitrification ($P_{14}n$) and nitrifier denitrification (uncounted in IPT_{anaN_2O}). The first two have been considered in IPT_{anaN_2O}. In terms of nitrifier denitrification, if the substrate NO_2^- is sourced purely from intracellular ammonia oxidation (i.e., unlabeled NH_4^+), then the product N_2O should be incorporated into the $P_{14}n$ estimation. However, if extracellular NO_2^- (i.e., $^{15}NO_2^-$) is involved in the reaction, "hybridized" $^{45}N_2O$ will be produced with one N atom from NH_4^+ and the other from $^{15}NO_2^-$. The production of this additional "hybridized" $^{45}N_2O$ will result in the decrease of qN_2O (i.e., increase r_{14-N_2O}). When "hybridized" $^{45}N_2O$ contributes an appreciable fraction of the $^{15}N_2O$, the slope of qN_2 against qN_2O will shift toward 1 or even larger than 1 and cause a significant underestimation in *ra*. Our field experiment showed no sign of influence by "hybridized" $^{45}N_2O$. The *ra* of 23 % estimated from intact sediment cores (Fig. 5) agrees well with that from slurry incubation (20 %). This observation can be explained in two ways: either the influence of the "hybridized" $^{45}N_2O$ in the *ra* estimation is equal in the suboxic environment (sediment cores) and the anoxic environment (slurry) or, more likely, the influence of the nitrifier denitrification is insignificant. Currently, our understanding of nitrifier denitrification in natural environments is limited, though Wrage et al. (2005) proposed a dual-isotope labeling method to quantify N_2O production from nitrifier denitrification in soil. However, the isotope technique cannot be used to identify "hybridized" $^{45}N_2O$ in the field.

Codenitrification is an alternative pathway to form hybridized N_2O or hybridized N_2, in which one N atom of nitrite (traceable by $^{15}NO_3^-$ addition) or nitric oxide combines via a nitrosyl intermediate with one N atom of another N species (e.g., amino acid) in N-nitrosation reaction (Tanimoto et al., 1992). The first field evidence in soil provided by Spott et al. (2011) by using ^{15}N tracers and a binomial model demonstrated the existence of codenitrification; however, this pathway on nitrogen cycling is still unclear in aquatic environments. Since the hybridized N_2O composes of one traceable ^{15}N species and one untraceable ^{14}N species during codenitrification, the isotope effect of this pathway should be similar to that found in the nitrifier denitrification in the IPT experiment. In other words, the slope of qN_2 against qN_2O would be larger than 1 if codenitrification predominates over anammox. Erler et al. (2008) reported only one case of a slope larger than 1 in a constructed wetland, which might be attributed to indistinguishable nitrifier denitrification or codenitrification.

Finally, the metabolism of benthic microalgae may also affect nitrogen removal rates by producing O_2, competing nutrients or even conduct N_2 fixation. Photosynthetic oxygen production has been found to reduce denitrification of nitrate supplied from the water column but to stimulate the coupled nitrification–denitrification in both light and dark incubations (Risgaard-Petersen et al. 1994). A similar result was found in Rysgaard et al. (1995), with exceptions in summer, when competition occurred between algal and bacterial assimilation. Although our method was not tested under light conditions, which is not the scope of current paper, we believe it is still applicable. Moreover, the applicability of IPT has been proved in many studies (e.g., Dong et al., 2000; Dunn et al., 2012; Pind et al., 1997; Sundbäck et al., 2000). In environments where N_2 fixation coexists with denitrification, such as coastal sediments covered by microbial mats or seagrass beds, the rate of denitrification will be underestimated (net production) due to the consumption of N_2 via synchronous N fixation if based on the measurement of $^{15}N_2$ production. An et al. (2001) proposed a modified $IPT_{classic}$ to quantify both processes at the same time. However, since N_2 fixation does not produce or consume N_2O, the calculations related to N_2O should not be affected. More studies should be done in future to test the applicability of our modified IPT; nevertheless, our

IPT method moves one step forward. This advance may be helpful to explore controlling factors of nitrate removal and differentiate interactive processes in various environments.

5 Conclusions and implications

Our study improved the existing methods for measuring nitrogen removal pathways in two aspects. First, we proposed the IPT_{anaN_2O} method in order to accurately quantify gas production from various pathways. Secondly, our instrumental modification allows for simultaneous accurate measurements of the two important ^{15}N-labeled gases sourced from the same sample vial, which considerably reduces analytical work. The results of field experiments derived from different versions of IPT revealed that IPT_{anaN_2O} is more reliable in environments characterized by the coexistence of high N_2O flux.

In addition, our instrumental modification is potentially applicable to high-frequency online measurements of ^{15}N gaseous production in the flow-through system (Rysgaard et al., 1994), operating under steady-state conditions for days to weeks, and could be beneficial to studies on parallel processes such as assimilation, nitrification and mineralization.

Since IPT_{anaN_2O} is capable of quantifying N_2O yield from denitrification and N_2O production from nitrification, this technique is particularly useful for exploring the mechanisms that regulate benthic N_2O flux. This research direction is crucial to understanding the possible changes of N_2O emissions in the context of growing coastal eutrophication and the hypoxic areas expansion caused by excessive nitrogen loading.

Appendix A

Equivalence of Eqs. (13) and (15)

Below, we prove that the Eq. (13) is equal to Eq. (15). First of all, Eq. (15) can be rewritten as the following equation, which represents an individual datum point instead of a slope from pooled data (Trimmer and Nicholls, 2009):

$$ra = \frac{2 - 2 \cdot \frac{q_{N_2}}{q_{N_2O}}}{2 - \frac{q_{N_2}}{q_{N_2O}}}. \quad \text{(A1)}$$

On the other hand, Eq. (13) is

$$ra = \frac{A_{14}}{D'_{14-N_2} + A_{14}}. \quad \text{(A2)}$$

By substituting D'_{14} and A_{14} with Eqs. (5) and (6), respectively, we can express *ra* as

$$ra = \frac{P_{29} - 2 \cdot r_{14-N_2O} \cdot P_{30}}{P_{29} + P_{30} \cdot \left(1 - r_{14-N_2O}\right)}. \quad \text{(A3)}$$

Since P_{29}/P_{30} is equal to $2 \cdot r_{14-N_2O}$, the *ra* can be expressed in terms of r_{14} after the numerator and the denominator are divided by P_{30}, which is

$$ra = \frac{2 \cdot r_{14-N_2} - 2 \cdot r_{14-N_2O}}{2 \cdot r_{14-N_2} - r_{14-N_2O} + 1}. \quad \text{(A4)}$$

Substituting r_{14} with q using Eq. (14) produces Eq. (A1).

Appendix B

Discussions of assumptions 5 and 6

Assumption 5 assumes that NO_3^- reduction is the only source of NO_2^- in the anoxic sediment layer. That is, supplies from other potential sources, such as NO_2^- from ammonia oxidation or downward diffusion from overlying water, are insignificant. Under this assumption, the fraction of ^{15}N in nitrite will be equal to that of nitrate. This assumption is indispensable for all versions of IPT; however, it is difficult to test specifically via IPT itself (see below). Several studies specifically focusing on NO_2^- production showed that NO_2^- in anoxic sediment mainly results from NO_3^- reduction (De Beer, 2000; Meyer et al., 2005; Stief et al., 2002), which supports this assumption. Although it is untestable via IPT itself, some phenomena caused by the violation of the assumption can be recognized through slurry incubation.

Conditions of high anammox activity and significant NO_2^- supply from nonlabeled sources to anammox will result in inconsistent outcomes between incubations of intact core and slurry sediment. For example, significant anammox activity can be revealed in slurry incubation after adding $^{15}NH_4^+$; at the same time, a positive correlation between values of $D_{14-\text{classic}}$ and $^{15}NO_3^-$ concentrations should be obtained from the intact core experiment if all NO_2^- comes from labeled sources (e.g., Fig. 7c). However, if NO_2^- is largely supplied from nonlabeled sources, then a constant value of $D_{14-\text{classic}}$ will be obtained in the $^{15}NO_3^-$ concentration series experiment because N_2 produced from anammox will be supported by non labeled NO_2^-. Note that the violation of assumption 6 below might result in the same inconsistency.

In general, nitrification that uses NH_4^+ as the substrate will not be affected by the addition of $^{15}NO_3^-$ (assumption 6). However, an indirect effect might occur in the NO_3^- addition experiment since high $^{15}NO_3^-$ concentrations may stimulate benthic microalgae (BMA) and/or anammox activity to deplete NH_4^+, thus limiting nitrification. Considering an environment without anammox, reduced nitrification might happen once BMA production is stimulated by the addition of $^{15}NO_3^-$. Such enhanced BMA may decrease coupled nitrification–denitrification ($P_{14}n$). Apparently, the underestimation of $P_{14}n$ causes an underestimate of $D_{14-\text{classic}}$ with the increase of $^{15}NO_3^-$ concentrations. However, if the growth of BMA does not result in reduction of nitrification,

$D_{14-\text{classic}}$ is expected to be independent of $^{15}NO_3^-$ additions, and thus a negative correlation between values of $D_{14-\text{classic}}$ and $^{15}NO_3^-$ concentrations should theoretically be obtained from an intact core incubated under light conditions. By comparing $D_{14-\text{classic}}$ responses between the light and dark incubations, the violation of assumption 6 due to BMA growth can be proved and distinguished with the violation of assumption 5.

Besides BMA, anammox is another process that might cause a nitrification underestimate. Similar to the effect of BMA, this in turn diminishes the NO_3^- supply, resulting in an underestimation of $P_{14}n$ and subsequently $D_{14-\text{classic}}$. Higher $^{15}NO_3^-$ additions will possibly cause a larger degree of underestimation in $D_{14-\text{classic}}$. In contrast, if this is the case, then anammox must be traceable. In other words, the $^{29}N_2$ produced from anammox will cause the overestimation of $D_{14-\text{classic}}$. This overestimation of $D_{14-\text{classic}}$ also grows with increased additions of $^{15}NO_3^-$. If both anammox and BMA coexist, then the underestimation of $D_{14-\text{classic}}$ caused by diminishing nitrification is compensated by stimulating anammox in different $^{15}NO_3^-$ treatments. Such compensation blocks a good positive correlation between $D_{14-\text{classic}}$ and the concentration spike of $^{15}NO_3^-$; more seriously, the positive correlation may even turn into negative correlation. Coupled with significant anammox activity observed in slurry incubation by adding NH_4^+, phenomena observed here thus resemble that caused by the violation of assumption 5. In addition, the degree of compensation might respond differently in light and dark incubation, and the difference can be used to reveal the competition of BMA and the nitrifiers and also to check the violation of assumption 6.

Supplementary material related to this article is available online at http://www.biogeosciences.net/10/7847/2013/bg-10-7847-2013-supplement.pdf.

Acknowledgements. Special thanks go to Mark Trimmer and the anonymous reviewer for constructive comments. This research was supported by the National Science Council, Taiwan (NSC 100-2621-M-001-003-MY3), and the National Natural Science Foundation of China (NSFC 41176059 and B07034).

Edited by: J. Middelburg

References

An, S., Gardner, W., and Kana, T.: Simultaneous measurement of denitrification and nitrogen fixation using isotope pairing with membrane inlet mass spectrometry analysis, Appl. Environ. Microbiol., 67, 1171–1178, 2001.

Bange, H. W.: New directions: the importance of oceanic nitrous oxide emissions, Atmos. Environ., 40, 198–199, 2006.

Bange, H. W., Rapsomanikis, S., and Andreae, M. O.: Nitrous oxide in coastal waters, Global Biogeochem. Cy., 10, 197–207, 1996.

Bergsma, T. T., Ostrom, N. E., Emmons, M., and Robertson, G. P.: Measuring simultaneous fluxes from soil of N_2O and N_2 in the field using the ^{15}N-gas "nonequilibrium" technique, Environ. Sci. Technol., 35, 4307–4312, 2001.

Brandes, J. A., Boctor, N. Z., Cody, G. D., Cooper, B. A., Hazen, R. M., and Yoder, H. S.: Abiotic nitrogen reduction on the early Earth, Nature, 395, 365–367, 1998.

Brandes, J. A., Devol, A. H., and Deutsch, C.: New developments in the marine nitrogen cycle, Chem. Rev., 107, 577–589, 2007.

Crowe, S. A., Canfield, D. E., Mucci, A., Sundby, B., and Maranger, R.: Anammox, denitrification and fixed-nitrogen removal in sediments from the Lower St. Lawrence Estuary, Biogeosciences, 9, 4309–4321, doi:10.5194/bg-9-4309-2012, 2012.

Dalsgaard, T., Nielsen, L. P., Brotas, V., Viaroli, P., Underwood, G. J. C., Nedwell, D. B., Sundback, K., Rysgaard, S., Miles, A., and Bartoli, M.: Protocol handbook for NICE-Nitrogen Cycling in Estuaries, National Environmental Research Institute, Copenhagen, Denmark, 2000.

Davidson, E. A.: Sources of nitric oxide and nitrous oxide following wetting of dry soil, Soil Sci. Soc. Am. J., 56, 95–102, 1992.

De Beer, D.: Potentiometric microsensors for *in situ* measurements in aquatic environments, in: In situ monitoring of aquatic systems: chemical analysis and speciation, edited by: Buffle, J. and Horvai, G., Wiley, 161–194, 2000.

Devol, A. H.: Denitrification including anammox, in: Nitrogen in the Marine Environment, 2nd ed., edited by: Capone, D., Bronk, D., Mulholland, M., and Carpenter, E., Elsevier, Amsterdam, 263–301, 2008.

Dong, L. F., Thornton, D. C. O., Nedwell, D. B., and Underwood, G. J. C.: Denitrification in sediments of the River Colne estuary, England, Mar. Ecol.-Prog. Ser., 203, 109–122, 2000.

Dong, L. F., Nedwell, D. B., and Stott, A.: Sources of nitrogen used for denitrification and nitrous oxide formation in sediments of the hypernutrified Colne, the nutrified Humber, and the oligotrophic Conwy estuaries, United Kingdom, Limnol. Oceanogr., 51, 545–557, 2006.

Dong, L. F., Smith, C. J., Papaspyrou, S., Stott, A., Osborn, A. M., and Nedwell, D. B.: Changes in benthic denitrification, nitrate ammonification, and anammox process rates and nitrate and nitrite reductase gene abundances along an estuarine nutrient gradient (the Colne Estuary, United Kingdom), Appl. Environ. Microb., 75, 3171–3179, 2009.

Dong, L. F., Naqasima-Sobey, M., Smith, C. J., Rusmana, I., Phillips, W., Stott, A., Osborn, A. M., and Nedwell, D. B.: Dissimilatory reduction of nitrate to ammonium, not denitrification or anammox, dominates benthic nitrate reduction in tropical estuaries, Limnol. Oceanogr., 56, 279–291, 2011.

Dunn, R. J. K., Welsh, D. T., Jordan, M. A., Waltham, N. J., Lemckert, C. J., and Teasdale, P. R.: Benthic metabolism and nitrogen dynamics in a sub-tropical coastal lagoon: Microphytobenthos stimulate nitrification and nitrate reduction through photosynthetic oxygen evolution, Estuar. Coast. Shelf Sci., 113, 272–282, 2012.

Erler, D., Eyre, B., and Davison, L.: The contribution of anammox and denitrification to sediment N_2 production in a surface flow constructed wetland, Environ. Sci. Technol., 42, 9144–9150, 2008.

García-Ruiz, R., Pattinson, S. N., and Whitton, B. A.: Denitrification and nitrous oxide production in sediments of the Wiske, a lowland eutrophic river, Sci. Total Environ., 210, 307–320, 1998a.

García-Ruiz, R., Pattinson, S. N., and Whitton, B. A.: Kinetic parameters of denitrification in a river continuum, Appl. Environ. Microbiol., 64, 2533–2538, 1998b.

Groffman, P. M., Altabet, M. A., Böhlke, J. K., Butterbach-Bahl, K., David, M. B., Firestone, M. K., Giblin, A. E., Kana, T. M., Nielsen, L. P., and Voytek, M. A.: Methods for measuring denitrification: diverse approaches to a difficult problem, Ecol. Appl., 16, 2091–2122, 2006.

Jäntti, H. and Hietanen, S.: The effects of hypoxia on sediment nitrogen cycling in the Baltic Sea, AMBIO, 41, 161-169, 2012.

Jensen, K. M., Jensen, M. H., and Kristensen, E.: Nitrification and denitrification in Wadden Sea sediments (Konigshafen, Island of Sylt, Germany) as measured by nitrogen isotope pairing and isotope dilution, Aquat. Microb. Ecol., 11, 181–191, 1996.

Joye, S. B., and Anderson, I. C.: Nitrogen cycling in coastal sediments, in: Nitrogen in the Marine Environment, 2nd ed., edited by: Capone, D. G., Bronk, D. A., Mulholland, M. R., and Carpenter, E. J., Academic Press, Amsterdam, 868–915, 2008.

Liss, P. S. and Slater, P. G.: Flux of gases across the air-sea interface, Nature, 247, 181–184, 1974.

Lohse, L., Kloosterhuis, H. T., Van Raaphorst, W., and Helder, W.: Denitrification rates as measured by the isotope pairing method and by the acetylene inhibition technique in continental shelf sediments of the North Sea, Mar. Ecol-Prog. Ser., 132, 169–179, 1996.

Luther, G. W., Sundby, B., Lewis, B. L., Brendel, P. J., and Silverberg, N.: Interactions of manganese with the nitrogen cycle: alternative pathways to dinitrogen, Geochim. Cosmochim. Ac., 61, 4043–4052, 1997.

Master, Y., Shavit, U., and Shaviv, A.: Modified isotope pairing technique to study N transformations in polluted aquatic systems: Theory, Environ. Sci. Technol, 39, 1749–1756, 2005.

Mcllvin, M. R., and Casciotti, K. L.: Fully automated system for stable isotopic analyses of dissolved nitrous oxide at natural abundance levels, Limnol. Oceanogr. Methods, 8, 54–66, 2010.

Meyer, R. L., Risgaard-Petersen, N., and Allen, D. E.: Correlation between anammox activity and microscale distribution of nitrite in a subtropical mangrove sediment, Appl. Environ. Microb., 71, 6142–6149, 2005.

Middelburg, J. J., Soetaert, K., and Herman, P. M. J.: Evaluation of the Nitrogen Isotope-Pairing Method for Measuring Benthic Denitrification: A Simulation Analysis, Limnol. Oceanogr., 41, 1839–1844, 1996a.

Middelburg, J. J., Soetaert, K., and Herman, P. M. J.: Reply to the Comment by Nielsen et al, Limnol. Oceanogr., 41, 1846–1847, 1996b.

Minjeaud, L., Bonin, P. C., and Michotey, V. D.: Nitrogen fluxes from marine sediments: quantification of the associated co-occurring bacterial processes, Biogeochemistry, 90, 141–157, 2008.

Mulder, A., Graaf, A. A., Robertson, L. A., and Kuenen, J. G.: Anaerobic ammonium oxidation discovered in a denitrifying fluidized bed reactor, FEMS Microbiol. Ecol., 16, 177–184, 1995.

Naqvi, S. W. A., Bange, H. W., Farías, L., Monteiro, P. M. S., Scranton, M. I., and Zhang, J.: Marine hypoxia/anoxia as a source of CH_4 and N_2O, Biogeosciences, 7, 2159–2190, doi:10.5194/bg-7-2159-2010, 2010.

Nielsen, L. P.: Denitrification in sediment determined from nitrogen isotope pairing, FEMS Microbiol. Lett., 86, 357–362, 1992.

Nielsen, L. P., Risgaard-Petersen, N., Rysgaard, S., and Blackburn, T. H.: Reply to the Note by Middelburg et al., Limnol. Oceanogr., 41, 1845–1846, 1996.

Pind, A., Risgaard-Petersen, N., and Revsbech, N. P.: Denitrification and microphytobenthic NO_3^- consumption in a Danish lowland stream: Diurnal and seasonal variation, Aquat. Microb. Ecol., 12, 275–284, 1997.

Poth, M., and Focht, D. D.: ^{15}N kinetic analysis of N_2O production by *Nitrosomonas europaea*: an examination of nitrifier denitrification, Appl. Environ. Microb., 49, 1134–1141, 1985.

Risgaard-Petersen, N., Rysgaard, S., Nielsen, L. P., and Revsbech, N. P.: Diurnal variation of denitrification and nitrification in sediments colonised by benthic microphytes, Limnol. Oceanogr., 39, 573–579, 1994.

Risgaard-Petersen, N., Nielsen, L. P., Rysgaard, S., Dalsgaard, T., and Meyer, R. L.: Application of the isotope pairing technique in sediments where anammox and denitrification coexist, Limnol. Oceanogr.-Methods, 1, 63–73, 2003.

Risgaard-Petersen, N., Meyer, R. L., Schmid, M., Jetten, M. S. M., Enrich-Prast, A., Rysgaard, S., and Revsbech, N. P.: Anaerobic ammonium oxidation in an estuarine sediment, Aquat. Microb. Ecol., 36, 293–304, 2004.

Rysgaard, S., Risgaard-Petersen, N., Sloth, N. P., Jensen, K., and Nielsen, L. P.: Oxygen regulation of nitrification and denitrification in sediments, Limnol. Oceanogr., 39, 1643–1652, 1994.

Seitzinger, S. P. and Kroeze, C.: Global distribution of nitrous oxide production and N inputs in freshwater and coastal marine ecosystems, Global Biogeochem. Cy., 12, 93–113, 1998.

Simon, J.: Enzymology and bioenergetics of respiratory nitrite ammonification, FEMS Microbiol. Rev., 26, 285–309, doi:10.1111/j.1574-6976.2002.tb00616.x, 2002.

Smith, M. S.: Dissimilatory Reduction of NO_2^- to NH_4^+ and N_2O by a Soil *Citrobacter* sp., Appl. Environ. Microb., 43, 854–860, 1982.

Smith, M. S. and Zimmerman, K.: Nitrous oxide production by non-denitrifying soil nitrate reducers, Soil Sci. Soc. Am. J., 45, 865–871, 1981.

Spott, O. and Stange, C. F.: Formation of hybrid N_2O in a suspended soil due to co- denitrification of NH_2OH, J. Plant Nutr. Soil Sci., 174, 554–567, 2011.

Spott, O., Russow, R., Apelt, B., and Stange, C. F.: A ^{15}N-aided artificial atmosphere gas flow technique for online determination of soil N_2 release using the zeolite Köstrolith SX6®, Rapid Commun. Mass Sp., 20, 3267–3274, 2006.

Stevens, R. J., Laughlin, R. J., Atkins, G. J., and Prosser, S. J.: Automated determination of nitrogen-15-labeled dinitrogen and nitrous oxide by mass spectrometry, Soil Sci. Soc. Am. J., 57, 981–988, 1993.

Stief, P., Beer, D., and Neumann, D.: Small-scale distribution of interstitial nitrite in freshwater sediment microcosms: the role of nitrate and oxygen availability, and sediment permeability, Microb. Ecol., 43, 367–377, 2002.

Strous, M., Heijnen, J. J., Kuenen, J. G., and Jetten, M. S. M.: The sequencing batch reactor as a powerful tool for the study

of slowly growing anaerobic ammonium-oxidizing microorganisms, Appl. Microbiol. Biot., 50, 589–596, 1998.

Sundbäck, K., Miles, A., and Göransson, E.: Nitrogen fluxes, denitrification and the role of microphytobenthos in microtidal shallow-water sediments: an annual study, Mar. Ecol.-Prog. Ser., 200, 59–76, 2000.

Tanimoto, T., Hatano, K., Kim, D., Uchiyama, H., and Shoun, H.: Co-denitrification by the denitrifying system of the fungus Fusarium oxysporum, FEMS Microbiol. Lett., 93, 177–180, 1992.

Thamdrup, B. and Dalsgaard, T.: Production of N_2 through anaerobic ammonium oxidation coupled to nitrate reduction in marine sediments, Appl. Environ. Microb., 68, 1312–1318, 2002.

Trimmer, M. and Nicholls, J. C.: Production of nitrogen gas via anammox and denitrification in intact sediment cores along a continental shelf to slope transect in the North Atlantic, Limnol. Oceanogr., 54, 577–589, 2009.

Trimmer, M., Risgaard-Petersen, N., Nicholls, J. C., and Engström, P.: Direct measurement of anaerobic ammonium oxidation (anammox) and denitrification in intact sediment cores, Mar. Ecol.-Prog. Ser., 326, 37–47, 2006.

van de Graaf, A. A., de Bruijn, P., Robertson, L. A., Jetten, M. S. M., and Kuenen, J. G.: Metabolic pathway of anaerobic ammonium oxidation on the basis of ^{15}N studies in a fluidized bed reactor, Microbiol., 143, 2415–2421, 1997.

Welsh, D., Castadelli, G., Bartoli, M., Poli, D., Careri, M., de Wit, R., and Viaroli, P.: Denitrification in an intertidal seagrass meadow, a comparison of ^{15}N-isotope and acetylene-block techniques: dissimilatory nitrate reduction to ammonia as a source of N_2O?, Mar. Biol., 139, 1029–1036, 2001.

Wrage, N., Velthof, G. L., Van Beusichem, M. L., and Oenema, O.: Role of nitrifier denitrification in the production of nitrous oxide, Soil Biol. Biochem., 33, 1723–1732, 2001.

Wrage, N., Groenigen, J. W. v., Oenema, O., and Baggs, E. M.: A novel dual-isotope labelling method for distinguishing between soil sources of N_2O, Rapid Commun. Mass Sp., 19, 3298–3306, doi:10.1002/rcm.2191, 2005.